Predicting triggering and consequence of delayed LNG RPT

Eskil Aursand[a,*], Morten Hammer[b]

[a] *Department of Energy and Process Engineering, Norwegian University of Science and Technology (NTNU), Trondheim N-7491, Norway*
[b] *SINTEF Energy Research, Sem Sælands vei 11, Trondheim NO-7034, Norway*

Abstract

We develop a model for delayed rapid phase transition (RPT) in LNG spills based on thermodynamics and nucleation theory which includes predictions of both triggering and vapor explosion consequence. We discover that the model predictions can be accurately characterized by two independent parameters alone: The initial fraction of methane and the molar mass of the remaining non-methane part. Based on this we develop correlations for risk assessment which may be used without access to the underlying advanced algorithms, and we give practical advice for risk mitigation. The model is consistent with an often reported empirical triggering criterion for cryogen RPT. We show that spilled LNG must typically boil down to about 10–20% of the original amount before RPT may occur, and after triggering one may expect energy yields of 10–20 g TNT per kg of triggered LNG. Explosive pressures in the range 20–60 bar can be expected.

Keywords: LNG, Rapid phase transition, Film boiling, Superheating, Thermodynamics

1. Introduction

Natural gas is a common fossil fuel mainly consisting of methane (CH_4) and with progressively smaller amounts of the heavier alkanes ethane (C_2H_6), propane (C_3H_8), butane (C_4H_{10}), etc. Some nitrogen may also be present. For the purposes of ship transport it is commonly cooled to form liquefied natural gas (LNG), a cryogen at about −162 °C. This is the hazardous material considered in this work.

In the LNG safety literature of the last couple of decades, the phenomenon called rapid phase transition (RPT) (Reid, 1983) is typically listed among the main concerns. This can range from giving it significant attention (Luketa-Hanlin, 2006; Shaw et al., 2005; Pitblado and Woodward, 2011; Cleaver et al., 2007), to little more than noting it as a concern (Alderman, 2005; Hightower et al., 2005; Havens and Spicer, 2007; Raj and Bowdoin, 2010; Forte and Ruf, 2017). The present work concerns the risk of RPT when LNG is spilled onto water, which is a possibility in maritime LNG operations, either during production, transportation, or usage. In such a spill, LNG will spread in a pool on the water surface while gradually boiling off, often without incident. However, in some cases it is observed to suddenly, and seemingly at random, explosively vaporize in large quantities at once. This is an RPT event, whose peak pressures and released mechanical energy can be large enough to displace and damage heavy equipment (Luketa-Hanlin, 2006; Pitblado and Woodward, 2011; Forte and Ruf, 2017) and could theoretically cause secondary structural damage and cascading containment failure (Havens and Spicer, 2007). Note that this is not an explosion in the common sense of the word, i.e. it does not involve combustion or other chemical reactions. It is what is sometimes called a vapor explosion or a physical explosion.

LNG has been transported in carriers at sea for roughly 50 years and is commonly stated to have an excellent safety record (Alderman, 2005; Forte and Ruf, 2017). However, there are still good reasons to

 https://doi.org/10.1016/j.jlp.2018.06.001
*Corresponding author
Email address: eskil.aursand@ntnu.no (Eskil Aursand)

address the issue of RPT risk: First, there is a record of actual unintended (though small scale) RPT-related incidents in the industry (Nédelka et al., 2003). Second, small accidents or near-accidents are not necessarily in the public record, so the risks may be higher than they appear to be. Third, the offshore activities of the LNG industry are growing more diverse. The use of LNG as a marine fuel is projected to increase significantly, which will lead to more small-scale bunkering operations. The industry is also moving towards increased use of floating facilities for production, storage, offloading and regasification (FPSO/FSRU) in order to make remote gas fields economically feasible (see emerging FLNG vessels). These developments introduce additional scenarios for LNG leakage, as well as potentially more severe consequences due to the addition of passengers, workers and more sensitive equipment. Such operations may not necessarily inherit the good safety record of the established LNG carrier operations. Overall, in the interest of preserving the excellent safety record of the industry, no significant theoretical risk should remain poorly understood.

Several research programs have been dedicated partly or fully to the subject of LNG RPT in the last few decades. The results and lessons from these projects have been thoroughly reviewed in the past (Cleaver et al., 1998; Nédelka et al., 2003; Luketa-Hanlin, 2006; Koopman and Ermak, 2007; Melhem et al., 2006). In parallel to this research, the RPT phenomenon has also received considerable attention in the context of fuel–coolant interactions in the nuclear power industry (Fletcher and Theofanous, 1994; Berthoud, 2000), which shares many of the same features. Overall, due to the small spatial scales (film boiling), small temporal scales (rapid nucleation) and poor reproducibility, exact quantification of LNG RPT risk and consequence has so far been elusive.

Models for RPT usually fall into one of two categories: Triggering prediction or consequence prediction. The former is concerned with then "if, when and where" of RPT, while the latter is concerned with the resulting energy yield and pressure peaks given that RPT does occur. LNG RPT triggering prediction have mostly been in the form of empirically based relationships between water temperature and thermodynamic properties of the LNG such as the superheat limit (Reid, 1983). Some more sophisticated methods have appeared in recent years (Melhem et al., 2006), based on gradual compositional change, but the details of the triggering criteria are not always clear. RPT consequence prediction is somewhat more mature. Thermodynamic methods to estimate the explosive yield of vapor explosions first appeared in the 1960s, in the context of nuclear fuel–coolant interactions. This is commonly referred to as the Hicks and Menzies (1965) method (Cleaver et al., 1998; Berthoud, 2000), and uses an idealized thermodynamic path of equilibration and isentropic expansion. While these methods may be applied directly to immediate RPT, that is not the case for delayed RPT due to the unknown LNG composition at the time of triggering.

Overall, the practical assessment of risk and consequence from a given LNG spill seems to still be unsettled, mostly due to the lack of reliable triggering prediction. A report made for the US Federal Energy Regulatory Commission in 2004 concluded that there was no satisfactory theoretical method for practical risk assessment of RPT in the case of LNG carriers (ABS Consulting, 2004). Still, a quite clear qualitative consensus has emerged in the literature regarding the mechanisms behind the RPT process:

1. Initially, after LNG spills on water, film boiling occurs. Since the heat transfer rate is limited, all the heat is spent on evaporation and the LNG stays in its quasi-equilibrium state while boiling (at the bubble point).
2. For some reason, film boiling collapse occurs, which suddenly increases the heat transfer rate by orders of magnitude. We call this the *triggering event*.
3. The sudden and large increase in heat transfer rate causes the liquid to superheat and then rapidly evaporate.
4. Since the vapor takes over 200 times as much space as the liquid, and the evaporation is so rapid, the event seems explosive in nature.

There is an established distinction in the literature between *early RPT* and *delayed RPT* in large scale LNG spills (Hightower et al., 2004; Luketa-Hanlin, 2006; Koopman and Ermak, 2007; Bubbico and Salzano, 2009). Early RPT triggers at the chaotic spill point at any time during the spill, while delayed RPT occurs in the outer parts of the spreading pool after considerable time has passed.

In the present work we concern ourselves with delayed RPT, whose probability appears to depend strongly on the composition of the LNG. While it has been shown that RPT will not occur with pure

methane (Enger et al., 1973; Porteous and Reid, 1976), they may occur with low-methane mixtures or with high-methane LNG mixtures who have had time to lose significant methane through boil-off (Luketa-Hanlin, 2006; Koopman and Ermak, 2007; Cleaver et al., 2007, 1998). In fact, it has been shown that usually a methane molar fraction below about 40% is necessary to make LNG-like mixtures experience RPT (Enger et al., 1973). This is much lower than the typical initial fraction of 90%, thus explaining the boil-off time necessary for delayed RPT. As we will show, the composition is important because it changes important parameters such as the Leidenfrost point (minimum temperature of film boiling) and the liquid superheat limit.

The focus of this work is to predict the risk and consequence of delayed RPT when spilling LNG on water. Underpinning this model are the following common hypotheses or assumptions regarding its mechanisms:

- The RPT event occurs if and only if the LNG is superheated to its superheat limit.
- Considerable superheating is only possible after film boiling collapse because it enables direct LNG–water contact.
- Film boiling collapse occurs due to the LNG's Leidenfrost temperature reaching the water temperature.
- The Leidenfrost temperature for saturated liquid-liquid film boiling depends only on the composition of the boiling fluid.

While it may be worth questioning these assumptions, that is outside the scope of this work. In this work, we take them at face value and follow them to their conclusions through the use of thermodynamic modelling and nucleation theory. Specifically, the assumptions lead to the following RPT triggering criterion,

$$T_{\mathrm{SHL}} < T_{\mathrm{w}} < T_{\mathrm{leid}}, \tag{1}$$

where T_{w} is the water temperature, T_{SHL} is the LNG superheat limit, and T_{leid} is the LNG Leidenfrost temperature. Here, we consider T_{w} to be constant and equal to the freezing temperature of water, since the water is cooled by the LNG but rarely forms ice (Luketa-Hanlin, 2006). The variables are T_{SHL} and T_{leid}, which both increase as methane is removed from the mixture during boil-off. The right hand side inequality in Eq. (1) expresses that film boiling collapse is necessary to superheat the LNG. The left hand side in equality in Eq. (1) expresses that the water must be hot enough to heat the LNG to the superheat limit.

Note that the distinction between delayed and early RPT lies in the last two assumptions listed above. In the present work *delayed* RPTs are defined as RPTs that are triggered due to purely thermodynamic changes leading to Eq. (1) being satisfied. Given this, delayed RPTs may occur in a completely undisturbed LNG pool on top of water. Any RPT events that occur before Eq. (1) is satisfied, such as due to external flow disturbances, are by the present definition *early* RPTs.

The theorized delayed RPT triggering event is illustrated in Fig. 1, which shows how we effectively move to the left along the boiling curve as methane boils off from the LNG mixture, eventually passing from film boiling to nucleate boiling. Note that the vertical axis in Fig. 1 is logarithmic, so the peak heat flux is actually several orders of magnitude larger than the heat flux at the Leidenfrost point.

Rather than presenting a radically new idea or theory for the RPT mechanism, the novelty of the present work lies in the following:

- The unification and refinement of leading theories for delayed LNG RPT, including both triggering and consequence models, into a single quantitative model. This model inherently takes into account the fact that the composition at the time of triggering is significantly different from the initial LNG compositon. The model also includes proper equation of state (EoS) thermodynamic modelling of mixtures, as opposed to the more common mole fraction average or ideal gas approaches.
- The use of this model to illustrate mechanisms behind triggering and expansion and to reveal a dependence on two independent parameters: The initial methane fraction, and the molar mass of the non-methane part.
- The mapping of simulation results throughout the entire relevant parameter space for LNG spills.

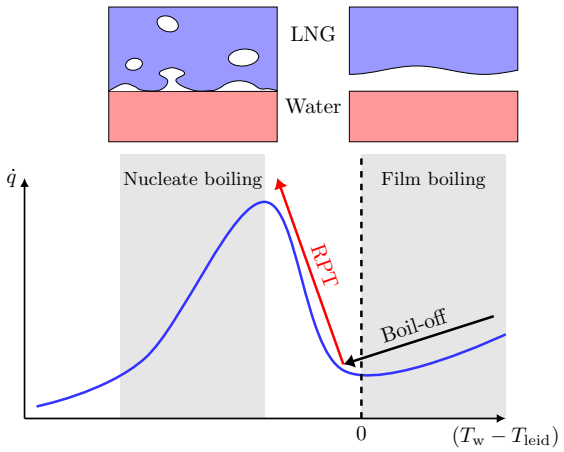

Figure 1: An illustration of the boiling curve, here as a plot of boiling heat flux ($\dot{q}$) against the difference between water temperature T_w and LNG Leidenfrost temperature T_{leid}. When T_w approaches T_{leid}, heat flux drops as we transition into the film boiling regime. When methane-rich LNG spills onto water, we initially have that $T_w \gg T_{leid}$. However, as the arrows show, when methane is removed from the mixture through boil-off T_{leid} is increased, which effectively moves us towards the left along the curve. Eventually the Leidenfrost point is crossed, film boiling breaks down, and RPT is triggered due to a sudden large increase in heat flux.

- The reduction of hundreds of simulation results into easy-to-use correlations that may be used for risk assessment without requiring access to advanced thermodynamic algorithms.

The most recent seemingly similar work is that of Benintendi and Rega (2014). The methods applied there are different in several ways, such as the use of correlations and mole fraction averaging instead of an EoS with mixture parameters. Their scope is also different, since they mostly consider the rapid fragmentation and evaporation of LNG droplets impacting the water and not long-term compositional change due to boil-off. Thus, their work mostly concerns early RPT, not delayed RPT as in the present work.

The present model is constructed as follows: In Sec. 2 we describe how the thermodynamic properties of the LNG mixture are modelled by the use of an equation of state (EoS). The thermodynamic model is the basis of both the RPT triggering prediction and the RPT consequence models, which are described in Sec. 3 and Sec. 4, respectively.

It is revealed that in this model both triggering and consequence is dependent on only two independent parameters. We show the general effect of changing them (Sec. 5) and how this knowledge may be used in practical assessment and mitigation of risk (Sec. 6). In Sec. 7 we illustrate the application of the model for an example case. In Sec. 8 we make sure that the model predictions are consistent with the sparse experimental data available before giving an overview of conclusions in Sec. 9.

2. Thermodynamics of multi-component fluids

2.1. Fundamental concepts

Thermodynamics properties were calculated by an *equation of state* (EoS), which is an equation relating the three state variables pressure, temperature and density for a homogeneous fluid phase. If the fluid is a mixture, such as LNG, the EoS has parameters that are composition dependent. For certain regions of parameter space, it turns out that the most stable (equilibrium) state is not a single phase but rather a state where the mass is split between one low density phase (vapor) and one high density phase (liquid). When working with a mixture, the two phases generally have different molar compositions. While all the information regarding these two-phase equilibrium states are technically contained within the EoS, finding

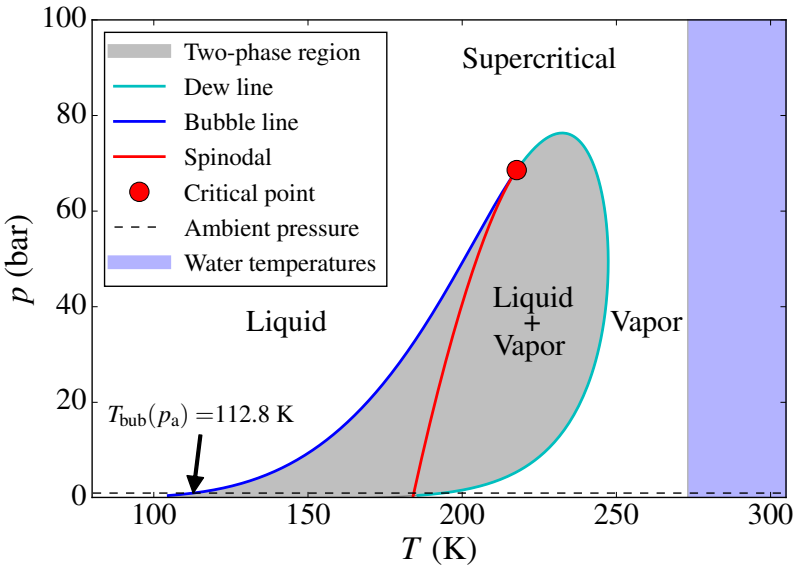

Figure 2: Phase diagram and spinodal of a typical natural gas composition, as predicted by the PR EoS. We especially identify the ambient pressure bubble point temperature, at about 113 K. For reference, on the right we also indicate the range of temperatures for liquid water.

these states requires a set of advanced multi-phase equilibrium algorithms (Michelsen and Mollerup, 2007; Wilhelmsen et al., 2017).

Given an EoS and an implementation of multi-phase equilibrium algorithms, it is possible to predict the equilibrium state of LNG given temperature (T), pressure (p) and an overall molar composition ($\boldsymbol{z}$). This yields a phase diagram, such as the one shown in Fig. 2. Note the following features:

- Two-phase region (gray shaded): Here the equilibrium state consists of two phases: A liquid phase and a vapor phase, generally of different compositions.
- Bubble line: Boundary between liquid region and two-phase region.
- Dew line: Boundary between vapor region and two-phase region.
- Critical point: Point where liquid and vapor properties merge.
- Spinodal: Maximum temperature where a superheated meta-stable liquid may theoretically exist. Sometimes called the *thermodynamic superheat limit*.

The topic of the spinodal requires some additional comments. While the gray shaded region in Fig. 2 indicates that the equilibrium state is two-phase, it is still possible to temporarily have a meta-stable purely liquid state in parts of this region. The spinodal marks the temperature limit beyond which it is impossible for this meta-stable liquid to exist.

2.2. Representing LNG

The LNG mixture was modelled as a mixture of the first four alkanes,

$$\boldsymbol{z} = [z_1, z_2, z_3, z_4], \tag{2}$$

where each number represents the molar fraction of methane (C1), ethane (C2), propane (C3), and n-butane (C4), respectively. The basic properties of these components are shown in Tab. 1. Any small amount of N_2 would not change the overall conclusions, since it would evaporate very quickly. Note that $\boldsymbol{z}$ is the given overall composition, and that in the the two-phase region the liquid and vapor would generally have different compositions.

Table 1: Basic properties of the alkanes considered in this work: Critical temperature (T_{crit}) and molar mass (M). Data from the NIST database (Linstrom and Mallard, 2017).

Name		T_{crit} (K)	M (kg mol^{-1})
Methane	("C1", CH_4)	191	0.01604
Ethane	("C2", C_2H_6)	305	0.03007
Propane	("C3", C_3H_8)	370	0.04410
n-Butane	("C4", C_4H_{10})	425	0.05812

2.3. Choice of EoS

The ISO Standard (ISO 20765-2/3) EoS for natural gas mixtures is the GERG-2008 (Kunz and Wagner, 2012) EoS, a highly accurate model applicable across a wide parameter space. However, it is a so-called multiparameter EoS (Span, 2010), which are very computationally demanding and comes with robustness challenges in relation to two-phase equilibrium algorithms, as discussed by Wilhelmsen et al. (2017). A faster and more robust alternative is a cubic equation of state, such as the Soave–Redlich–Kwong (SRK) (Soave, 1972) or Peng–Robinson (PR) (Peng and Robinson, 1976) equations. The cubic equations are quite good at predicting the two-phase region and the phase compositions therein but are known to have significant errors for the speed of sound and liquid densities at high pressures (Kunz and Wagner, 2012, Sec. 2.1.2). What mattered most in the present study was the location of the bubble line, critical point, and the ambient pressure spinodal. Due to this, the calculations were performed with the PR EoS.

3. RPT triggering model

The stated triggering criterion in Eq. (1) was central to predicting delayed RPT. As mentioned, T_{w} was considered constant (273.15 K), while T_{SHL} and T_{leid} were considered $\boldsymbol{z}$-dependent variables. For typical LNG compositions triggering is initially prevented because $T_{\text{leid}} < T_{\text{w}}$ (film boiling). However, as methane boils off from the mixture T_{leid} will increases until eventual film boiling collapse, which will cause sudden heating to the superheat limit if $T_{\text{w}} > T_{\text{SHL}}$. The key to prediction is thus to estimate the functions $T_{\text{leid}}(\boldsymbol{z})$ and $T_{\text{SHL}}(\boldsymbol{z})$ in order to find the composition ranges where triggering is possible.

3.1. Predicting the Leidenfrost temperature

As shown in Fig. 1, the Leidenfrost temperature T_{leid} is the surface temperature below which film boiling breaks down. A decent amount of experimental data for T_{leid} of pure fluids could be found in the literature, as summarized in Tab. 2. It has been suggested by authors such as Spiegler et al. (1963) that the Leidenfrost point can be estimated from

$$T_{\text{leid}} = \frac{27}{32} T_{\text{crit}}. \tag{3}$$

The data from Tab. 2 was compared with Eq. (3) in Fig. 3. The simple equation appeared to give an excellent prediction for methane, and generally a decent upper estimate for all the other fluids. Therefore, Eq. (3) was adopted as an estimate for the T_{leid} of LNG, using a computed critical point for any given mixture. Looking further into the mechanisms of film boiling collapse was deemed beyond the scope of this work.

Note that evaluating Eq. (3) for mixtures is significantly more complicated than for pure fluids. The critical point must be solved for with the combination of an EoS and an iterative algorithm, as opposed to simply looking up the pure fluid T_{crit} in a table.

Table 2: Overview of fluids where data could be found on the Leidenfrost point at ambient pressure. Here T_{leid} is the average of the N_{leid} data points found. Also shown is the ambient pressure saturation (boiling) temperature, and the critical temperature, as given by the NIST database (Linstrom and Mallard, 2017). The sources for Leidenfrost point data are Sakurai et al. (1990); Yao and Henry (1978); Gottfried and Bell (1966); Qiao and Chandra (1997); Bernardin and Mudawar (1999); Sakurai et al. (1990); Baumeister and Simon (1973); Nagai and Nishio (1996); Valencia-Chavez (1978); Vesovic (2007); Yao and Henry (1978); Berenson (1961).

Fluid	T_{sat}(K)	T_{leid}(K)	T_{crit}(K)	N_{leid}
Water	373.15	462.78	647.0	12
Nitrogen	77.36	100.00	126.2	7
Freon11	296.92	346.50	471.2	4
Freon113	320.74	378.03	482.9	5
Acetone	329.30	409.40	508.0	4
Methane	111.70	163.33	190.6	3
Ethanol	351.50	429.10	514.0	3
Pentane	309.21	367.00	469.8	1
Cyclohexane	353.89	438.15	554.0	1
Benzene	353.30	448.15	562.0	1

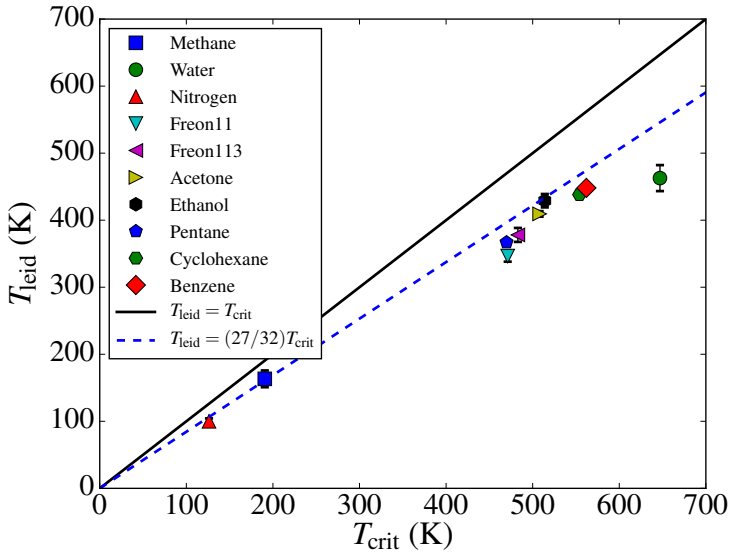

Figure 3: The experimental pure fluid Leidenfrost temperatures from Tab. 2 plotted against critical temperature. Also shown (dashed line) is the simple Leidenfrost temperature model in Eq. (3). Error bars represent spread of data in the cases where more than one data point was found.

3.2. Predicting the liquid superheat limit

As mentioned in Sec. 2, it is possible to superheat a liquid to a meta stable state beyond the bubble line, and the liquid spinodal is the theoretical limit to this superheating. However, as discussed by Aursand et al. (2017), in practice spontaneous homogeneous nucleation happens before reaching the spinodal due to the always present thermal fluctuations. The magnitudes of both the nucleation barrier and the fluctuations are temperature dependent, and the threshold temperature where the fluctuations become very likely to overcome the barrier is called the *(kinetic) superheat limit* (SHL).

As shown in Aursand et al. (2017), the superheat limit for alkanes, both pure and mixture, may be accurately estimated through classical nucleation theory (CNT). The basic principle is to estimate the probability of thermal fluctuations creating tiny vapor nuclei beyond a critical size, and this is represented by a classical Arrhenius rate law,

$$J = J_0 \exp\left(-\frac{\Delta G}{k_{\mathrm{B}} T}\right). \tag{4}$$

For pure fluids, the nucleation barrier is (Aursand et al., 2017)

$$\Delta G = \frac{16\pi\sigma^3(T)}{3\left(p_{\mathrm{sat}}(T) - p\right)^2}, \tag{5}$$

and the rate at zero nucleation barrier is

$$J_0 = \frac{\rho_{\mathrm{l}}}{m^{3/2}}\sqrt{\frac{2\sigma}{\pi}}. \tag{6}$$

Here, k_{B} is the Boltzmann constant, σ is the surface tension, p_{sat} is the saturation pressure at the given temperature, p is the actual pressure, ρ_{l} is the liquid density, and m is the mass of a single molecule. The expression for J_0 varies somewhat between sources, but this has a negligible effect on the predicted SHL.

The expression in Eq. (4) may only predict a nucleation rate. In order to find the SHL it was necessary to define a critical nucleation rate J_{crit} which corresponds to sudden macroscopic phase change. Due to the rapid growth of the exponential in Eq. (4), the result is quite insensitive to the specific choice of J_{crit}. In this work the value of $J_{\mathrm{crit}} = 1 \cdot 10^{12}\,\mathrm{s}^{-1}\mathrm{m}^{-3}$ was used, similar to previous works (Bernardin and Mudawar, 1999; Aursand et al., 2017). Thus, in order to predict the superheat limit, it was necessary to solve the implicit equation

$$J(T) = J_{\mathrm{crit}} \tag{7}$$

to yield T_{SHL}. However, due to the insensitivity to the values of J_0 and J_{crit}, the above could be simplified. Since $\ln(J_0/J_{\mathrm{crit}})$ is almost constant (≈ 64), one is past the critical nucleation rate when $\Delta G < 64 k_{\mathrm{B}} T$, and thus to a good approximation one could instead solve

$$\frac{\left(p_{\mathrm{sat}}(T) - p\right)^2 k_{\mathrm{B}} T}{\sigma^3(T)} = \frac{\pi}{12}, \tag{8}$$

for temperature. To solve Eq. (8) requires the surface tension function $\sigma(T)$ and an EoS to evaluate $p_{\mathrm{sat}}(T)$. Note that it is critical to include the temperature dependence of σ.

The above theory was developed for pure fluids. For mixtures, the bubble line pressure was substituted for the saturation-line pressure, and the mixture surface tension was calculated as a mole fraction weighted average of the surface tension of the pure components. The surface tension functions for the pure components were found by interpolating tables from the NIST database (Linstrom and Mallard, 2017).

It is interesting to see how the predicted SHL generally follows the thermodynamics quantities. From solving Eq. (8) at atmospheric pressure throughout the possible composition range, it was found that

$$T_{\mathrm{SHL}} \approx 0.95 T_{\mathrm{spin}} \quad (p = 1\,\mathrm{atm}), \tag{9}$$

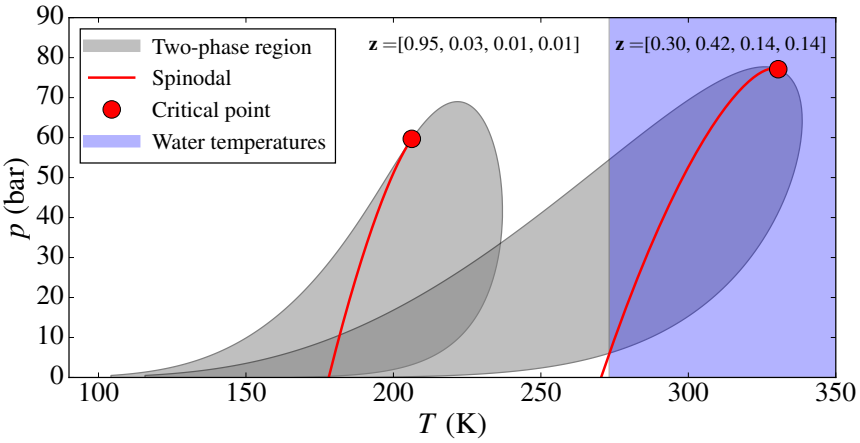

Figure 4: Illustration of how the phase diagram changes as methane is removed from the LNG mixture, and eventually enters the region of water temperatures. Calculations were made with the PR EoS. See Eq. (2) for interpretation of the composition vector $\mathbf{z}$.

regardless of composition. It was also found that the superheat limit loosely follows the critical temperature,

$$0.64T_{\text{crit}} < T_{\text{SHL}} < 0.89T_{\text{crit}} \quad (p = 1\,\text{atm})\,, \tag{10}$$

with the exact position within this interval depending on composition. Note from Eq. (1) that triggering is only possible if $T_{\text{SHL}} < T_{\text{leid}}$. When combining Eq. (3) with the average value from Eq. (10), it can be seen that typically $T_{\text{SHL}} \approx 0.9T_{\text{leid}}$.

3.3. Detecting triggering during boil-off

The aim was to simulate the long-term thermodynamic effect of LNG film boiling on top of water. Having time as the progress parameter of the boil-off would require the estimation of heat transfer rate and pool thickness, which was beyond the scope of this work. In the present work, the progress parameter was chosen to be the decreasing methane amount during boil-off. Based on this one may look for the methane fractions where the triggering criterion Eq. (1) is satisfied.

The vapor leaving the LNG will not have the same composition as the liquid, since the lighter components are more volatile. To a good approximation one may assume that only CH_4 molecules escape into the vapor during boiling (Enger et al., 1973). Given an original composition $\boldsymbol{z}^{(0)}$ and a current methane fraction z_1, the current composition vector $\boldsymbol{z}$ can be found from

$$z_i = z_i^{(0)} \frac{1 - z_1}{1 - z_1^{(0)}} \quad \forall \quad i > 1. \tag{11}$$

The above gives a linear increase in the fraction of the heavier alkanes as a function of the decreasing methane amount. This comes with a change in the thermodynamic properties of the LNG, generally shifting the two-phase region to higher temperatures, as shown in Fig. 4.

With the use of Eq. (11), all properties can be plotted as a function of methane fraction as shown in Fig. 5. Since both T_{leid} and T_{SHL} are now known as a function of z_1, the zone of z_1 values where the triggering criterion Eq. (1) is satisfied can be indicated (shaded red in Fig. 5). Note especially the highest methane fraction of this region, where $T_{\text{leid}} = T_{\text{w}}$, in this example about 0.4. This is denoted as z_{leid}, the *Leidenfrost fraction*. The corresponding composition vector is called the *Leidenfrost composition*.

Note that a plot such as Fig. 5 does not depend on initial methane fraction $z_1^{(0)}$. Changing the initial methane fraction simply corresponds to changing the starting position on the same plot. The plot (and

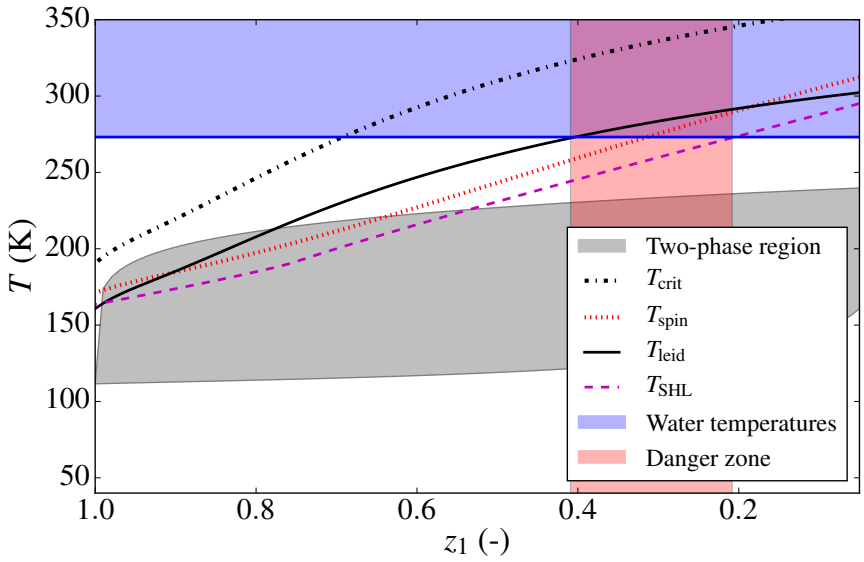

Figure 5: Properties changing as methane is removed from the mixture, for the case of $\tilde{\boldsymbol{z}} = [0.5, 0.3, 0.2]$. The composition region shaded in red is where the RPT triggering criterion Eq. (1) is satisfied. The methane fraction when entering this region is called the *Leidenfrost fraction*, which in this case is $z_{\text{leid}} \approx 0.4$. Then, when $z_1 < 0.2$, the superheat limit is so high that RPT will not occur even though film boiling has collapsed.

z_{leid}) does however depend on the composition of the non-methane part, which can be characterized by the *remainder composition*,

$$\tilde{\boldsymbol{z}} = \frac{1}{1 - z_1} [z_2, z_3, z_4], \tag{12}$$

which is constant during boil-off. While many results technically depend on every component in $\tilde{\boldsymbol{z}}$, it was found that many correlate strongly with a quantity $\eta(\tilde{\boldsymbol{z}})$, here called the *alkane factor*. The vector $\tilde{\boldsymbol{z}}$ maps to the scalar η by

$$\eta = \frac{[M_2, M_3, M_4] \cdot \tilde{\boldsymbol{z}}}{M_2}, \tag{13}$$

i.e. it is the molar mass of the non-methane part, relative to the molar mass of ethane. The value starts at $\eta = 1$ for C1+C2 only, and increases as more of heavier alkanes C3 and C4 is added. Typical values for LNG mixtures are between 1.1 and 1.4.

It is now assumed that triggering occurs immediately once the criterion Eq. (1) is satisfied so that the methane fraction at that moment is z_{leid}. Formally, z_{leid} must be found by iteratively searching for the value of z_1 that solves $T_{\text{leid}} = T_{\text{w}}$ and for every step this would require the iterative calculation of the mixture critical point. Thankfully, it was found that z_{leid} correlated strongly with the alkane factor η, as seen in Fig. 6. The following fit was found,

$$z_{\text{leid}} = 1 - \frac{0.36}{\eta - 0.73}, \tag{14}$$

which can be used for practical purposes.

Note the following features:

- Since η normally satisfies $\eta < 1.4$, z_{leid} is normally less than 0.5, i.e. the mixture needs to boil down to less than 50% methane in order to trigger RPT.

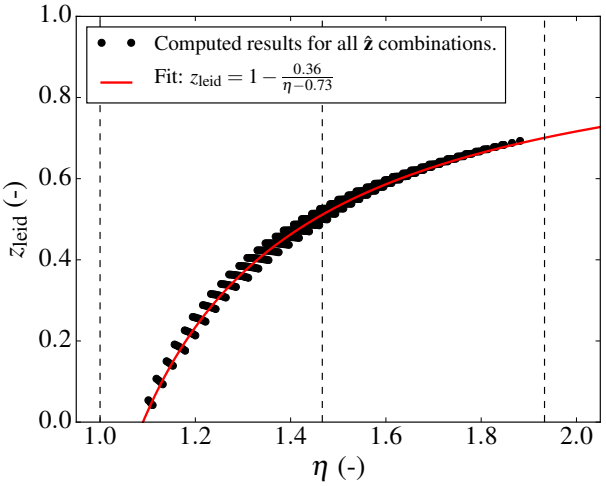

Figure 6: Calculated values of the Leidenfrost fraction z_{leid} plotted against the alkane factor η. The solid red line shows a functional fit (Eq. (14)), which crosses zero at $\eta = 1.09$. The vertical dashed line show the η values corresponding to pure ethane, propane, and butane, from left to right.

- If the initial mixture is close to being only methane and ethane ($\eta < 1.09$), it will never trigger. This is because the Leidenfrost temperature of the remainder composition is below the water temperature, so it doesn't matter if all the methane boils off.

While changing the initial methane fraction does not change the methane fraction needed for triggering (z_{leid}), it does change how much boil-off is necessary to reach it. The *reduction factor* r is defined as the moles of LNG remaining at triggering divided by the original moles of LNG spilled. It can be found from

$$r(z_1^{(0)}, z_{\text{leid}}) = \frac{1 - z_1^{(0)}}{1 - z_{\text{leid}}}, \quad \left(z_{\text{leid}} < z_1^{(0)} < 1.0\right), \tag{15}$$

where $z_1^{(0)}$ is the initial fraction of methane. By combining Eqs. (14) and (15), one may see that

$$r(z_1^{(0)}, \eta) = \left(1 - z_1^{(0)}\right)\left(\frac{\eta - 0.73}{0.36}\right). \tag{16}$$

4. RPT consequence model

After triggering (film boiling collapse), heat flux increases dramatically due to the transition into the nucleate boiling regime (see Fig. 1). Since the evaporation process is unable to absorb the sudden heat flux increase, the liquid superheats. Superheating proceeds until the superheat limit T_{SHL}, which can be found by solving Eq. (8) at ambient pressure (p_{a}) and the Leidenfrost composition. Once at the superheat limit the fluid will have to find its equilibrium state. This state contains a significant amount of vapor, and thus it takes up a much larger volume at ambient pressure. Since the transition is very rapid, it will go through an intermediate high pressure state, which gives the event its explosive effect.

The RPT consequence model in the present work was based on the established basic principles of Hicks and Menzies (1965). However, no assumptions of ideal gas were made in the thermal equilibration nor the expansion process. Note also that the input composition to this model was based on the result of the RPT triggering model (Leidenfrost compositon), and not simply set to the initial LNG compositon. In the present work, akin to the Hicks & Menzies methodology, the triggering and explosion processes were approximated by the following series of steps (see Fig. 7):

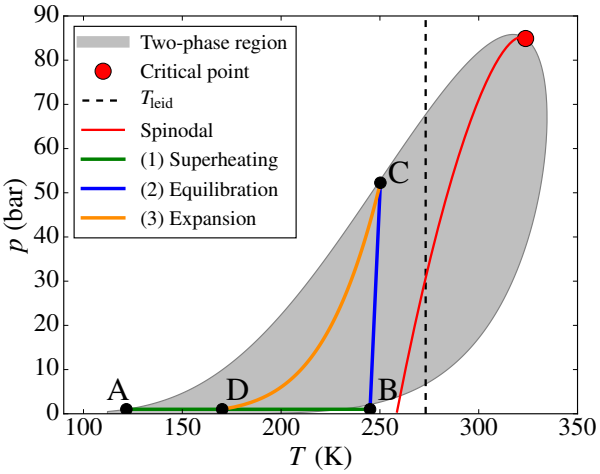

Figure 7: The thermodynamic path of triggering and explosion for an example value of $\tilde{\boldsymbol{z}}$. The states are labelled A through D according to the list in Sec. 4.

- **A** $(T_{\text{bub}}, p_{\text{a}})$: The state at the moment of triggering (film boiling collapse). This is a liquid equilibrium state on the bubble line. After triggering the liquid temperature suddenly increases.
- **B** $(T_{\text{SHL}}, p_{\text{a}})$: The superheat limit. This is a liquid non-equilibrium (meta-stable) state, which will rapidly expand to its corresponding equilibrium.
- **C** (T^*, p^*): A liquid–vapor quasi-equilibrium state. This is the thermodynamic equilibrium state with the same volume and energy as the meta-stable state B, and can be found using two-phase equilibrium algorithms together with an EoS. This state is mostly liquid, but its pressure p^* is much higher than the ambient. It is usually quite close to the bubble line but slightly inside the two-phase region. This is an equilibrium state given the volume and energy from B. This is called a quasi-equilibrium state because it is not in thermal or mechanical equilibrium with the surroundings.
- **D** $(T_{\text{end}}, p_{\text{a}})$: The equilibrium state resulting from an isentropic expansion from state C to ambient pressure. This state is mostly vapor, and has more than a hundred times the volume of the other states.

The above process is similar to the one that was suggested by Melhem et al. (2006), except that they placed B at the spinodal (not superheat limit) and simply determined C as the point on the bubble line with the same temperature as B.

In the present work the explosive energy yield per mole of triggered liquid (E) was estimated as the expansion work of C $\rightarrow$ D, which could be found from the enthalpy difference between the two states. The pressure of state C was used to approximate the maximum explosion pressure p^*.

Both E and p^* are functions of the remainder composition only, since the process A $\rightarrow$ D occurs at the Leidenfrost composition, not the initial composition. Once again it turned out that these results correlated strongly with the alkane factor η, as shown in Figs. 8 and 9. Functions of η fitted to these results were

$$\frac{E}{1\,\text{kJ mol}^{-1}} = 4.731\eta^3 - 24.65\eta^2 + 41.75\eta - 20.60, \tag{17}$$

and

$$\frac{p^*}{62\,\text{bar}} = 1 - \text{e}^{-5.6(\eta-1)}. \tag{18}$$

These correlations may be used in the range $\eta \in (1.0, 1.8)$, which is the range where most realistic cases were found to be in. The molar mass of the mixture during boil-off is a function of the changing methane

fraction z_1 and the constant alkane factor η,

$$M = z_1 M_1 + \eta(1 - z_1)M_2. \tag{19}$$

The mixture molar mass at triggering (M_{leid}) is thus a function of η alone, since there $z_1 = z_{\text{leid}}(\eta)$. From the molar mass one may find the yield per mass,

$$E^{(\text{mass})}(\eta) = \frac{E}{M_{\text{leid}}}, \tag{20}$$

which is plotted in Fig. 10. Note how $E^{(\text{mass})}$ only depends on η, not the initial methane fraction.

The values in Fig. 10 and Eq. (17) are explosive yield per mole of LNG present at the time of triggering. It is also interesting to know the potential explosive yield for a given spilled amount of LNG. On a molar basis, this may simply be found by multiplying E with the reduction factor r. Per mass of spilled LNG it becomes

$$E_0^{(\text{mass})}(\eta, z_1^{(0)}) = \frac{rE}{M_0}, \tag{21}$$

where M_0 is the molar mass of the initial mixture, i.e. Eq. (19) evaluated at $z_1 = z_1^{(0)}$. Note how $E_0^{(\text{mass})}$ depends on both η and $z_1^{(0)}$. Example results are shown in Fig. 11. Note that in contrast to Fig. 10, Fig. 11 shows that yield with respect to initial mass increases monotonously with η. This is due to the effect η has on the reduction factor r: Increasing η leads to earlier triggering so that more of the initial mass remains.

Note that the energy yield calculated here is from the combination of an isolated (B $\rightarrow$ C) and an isentropic (reversible) (C $\rightarrow$ D) process. Any other process will give irreversible loss of energy, so the present idealization will give an upper bound to the actual yield. It has been suggested that the actual yield is closer to 50% of this prediction (Melhem et al., 2006).

5. Discussion

5.1. RPT predictions

We have demonstrated how triggering and consequence of delayed LNG RPT may be affected by the following two independent properties of the initial LNG composition:

- **Alkane factor** (η): While the effects of the non-methane part are fully specified by the vector $\tilde{\boldsymbol{z}}$, we have shown that they can be accurately predicted through the corresponding scalar property η. This value represents how heavy the non-methane part of the LNG is, relative to the case of pure ethane.
- **Initial mole fraction of methane** ($z_1^{(0)}$): This value is found directly from the initial composition $\boldsymbol{z}^{(0)}$. Adding or removing methane does not affect η.

Overall, either reducing η or increasing $z_1^{(0)}$ will be beneficial to safety. Specifically, reducing η has the following effects:

- Reducing the explosive yield per initial mass ($E_0^{(\text{mass})}$), as shown in Fig. 11. This is mostly due to the reduction on the Leidenfrost fraction z_{leid} (Fig. 6), which in turn reduces the reduction factor r (Eq. (16)), i.e. there will be less total LNG remaining at the time of triggering. As seen in Fig. 10, the effect on the yield per *triggered* mass ($E^{(\text{mass})}$) is less clear-cut.
- Reducing the predicted maximum pressure of the RPT explosion (p^*), as shown in Fig. 9.

Increasing $z_1^{(0)}$ has the following effects:

- Reducing the explosive yield per initial mass, as shown in Fig. 11. This is mostly due to the effect of reducing the reduction factor r (Eq. (16)). It does not affect the yield per triggered mass ($E^{(\text{mass})}$).

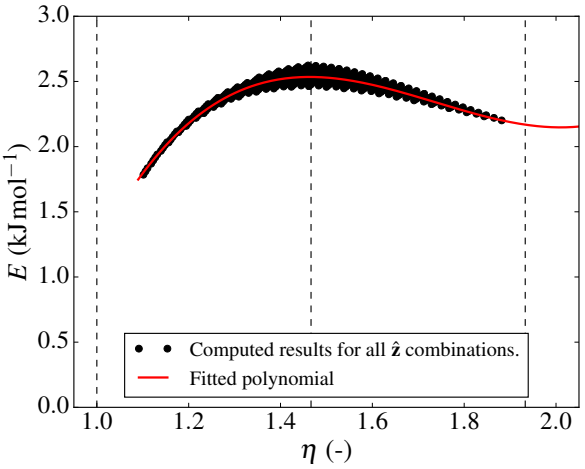

Figure 8: Calculated values for RPT explosive yield according to the expansion step illustrated in Fig. 7, throughout the space of possible $\tilde{\boldsymbol{z}}$, plotted against η. Also shown is the polynomial fit in Eq. (17).

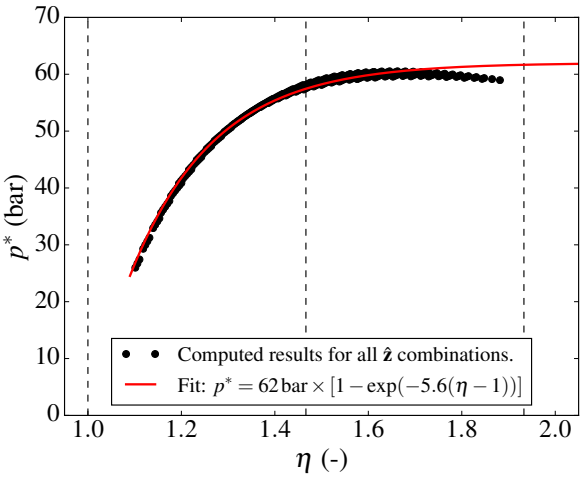

Figure 9: Calculated values for maximum RPT explosive pressure according to the pressure of point C in Fig. 7, throughout the space of possible $\tilde{\boldsymbol{z}}$, plotted against η. Also shown is the fit in Eq. (18).

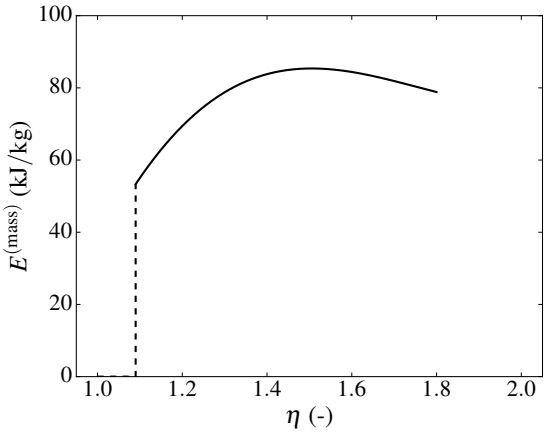

Figure 10: The RPT explosive yield per mass of LNG at time of triggering based on Eq. (20) Below $\eta = 1.09$ the yield effectively drops to zero, since even the remaining mixture at zero methane does not have a high enough Leidenfrost temperature to trigger.

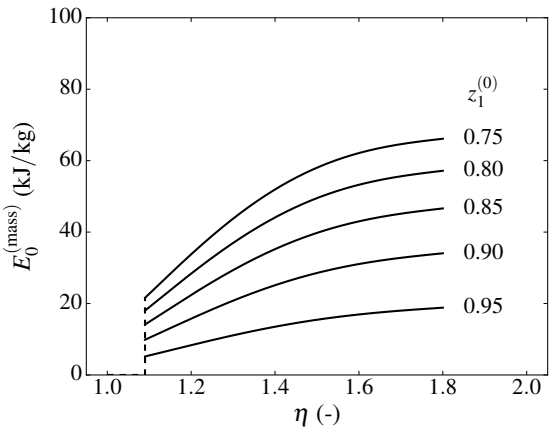

Figure 11: The RPT explosive yield per mass of *initial* LNG based on Eq. (21). Below $\eta = 1.09$ the yield effectively drops to zero, since even the remaining mixture at zero methane does not have a high enough Leidenfrost temperature to trigger.

5.2. Comments on early RPT

We may also ask what to expect of early RPT. While the triggering model in Sec. 3 is only for predicting delayed RPT, the consequence model in Sec. 4 still applies. The difference is that the calculation must be done on a mixture with much more methane than the Leidenfrost composition, since early RPT by definition occurs before that composition is reached. With a typical initial LNG composition as an extreme case, it was found that the maximum pressure is reduced to about 50% and that the yield (per triggered mass) is reduced to about 70%, compared to the corresponding delayed RPT event. This does not necessarily mean that the risk is less, since the total yield in a single early RPT event is not known. What is known is that the total potential explosive yield is actually higher, since there is 5–10 times more LNG available for early RPT due to the boil-off reduction factor.

5.3. Comments on model approximations

As with any model, the present one is an approximation and has certain weaknesses. A central approximation in the simulated boil-off is that we only allow methane to boil off, while the heavier alkanes stay in the liquid. This is a very good approximation as long as there is still significant methane amounts remaining in the liquid. An artifact of this approximation is that in the cases of $\eta < 1.09$ we predict that film boiling collapse will never happen, since the Leidenfrost temperature can never reach the water temperature. In reality significant ethane boil-off will commence once the methane is gone, and move the Leidenfrost temperature further up until eventual film boiling collapse. However, since we then know that the reduction factor will be very small ($r < 1 - z_1^{(0)}$), we consider the risk minimal when $\eta < 1.09$.

On the topic of film boiling collapse, the model is very much dependent on the assumption that the Leidenfrost point prediction in Eq. (3) is as accurate for mixtures as it is for pure fluids. However, without data on the Leidenfrost point of mixtures this cannot be confirmed.

Once film boiling collapses, superheat can commence, starting the transition from state A to state B (see Fig. 7). In this model, we assume that superheating proceeds until the superheat limit is reached, which is the point where homogeneous nucleation occurs due to thermal fluctuations, no matter how careful the heating is performed. However, in reality, external disturbances may cause phases transition to trigger before reaching this limit. In that case, we would expect both the yield and pressure to be lower, and in this sense the present model represents a worst-case estimate. Also, when finding the superheat limit it is necessary to evaluate some liquid properties outside the equilibrium region. Here we assume that the EoS reasonably extrapolates into the meta-stable region, despite mostly being fitted to equilibrium data.

6. Procedure for risk assessment and mitigation

We now present a procedure for practical risk assessment and mitigation which do not require access to advanced thermodynamic software and only uses the correlations developed in this work.

6.1. Predicting consequence

To estimate the worst-case RPT consequence of an LNG spill, perform the following procedure:

1. Find the initial mole fractions of alkanes, $\boldsymbol{z}^{(0)}$, and the molar mass of each component, M_i.
2. Calculate the following two parameters: The alkane factor η (through Eqs. (12) and (13)) and the initial methane fraction $z_1^{(0)}$ (first value in $\boldsymbol{z}^{(0)}$).
3. If $\eta > 1.09$:
   - Based on these two parameters, calculate reduction factor r (through Eq. (16)). This is the estimated fraction of initial LNG still present at the time of triggering.
   - Calculate the explosive yield per triggered LNG mass $E^{(\mathrm{mass})}$ from Eq. (20) and Eq. (17).
   - Calculate the explosive yield per initial LNG mass $E_0^{(\mathrm{mass})}$ from Eq. (21) and Eq. (17). If multiplied with total mass of spilled LNG, this represents the total potential explosive yield from RPT events, likely distributed between several blasts.
   - Calculate the maximum expected pressure from Eq. (18).

If $\eta < 1.09$, risk is considered minimal.

Table 3: An overview of model results in a given example case.

Input:			
$\boldsymbol{z}^{(0)}$	[0.90, 0.06, 0.03, 0.01]	Initial composition	
Results:			
$\tilde{\boldsymbol{z}}$	[0.6, 0.3, 0.1]	Remainder composition	Eq. (12)
η	1.23	Alkane factor	Eq. (13)
z_{leid}	0.285	Leidenfrost fraction	Eq. (14)
r	0.14	Reduction factor	Eq. (16)
M_0	$0.0181\,\mathrm{kg\,mol^{-1}}$	Initial molar mass	Eq. (19)
M_{leid}	$0.0311\,\mathrm{kg\,mol^{-1}}$	Molar mass at triggering	Eq. (19)
$E^{(\mathrm{mass})}$	$73\,\mathrm{kJ\,kg^{-1}}$	Yield per triggered mass	Eq. (20)
$E_0^{(\mathrm{mass})}$	$17\,\mathrm{kJ\,kg^{-1}}$	Yield per initial mass	Eq. (21)
p^*	45 bar	Maximum pressure of vapor-explosion	Eq. (18)

6.2. Reducing consequence

Risk can generally be reduced by either reducing η or increasing $z_1^{(0)}$, while keeping the other constant. One can also do both simultaneously.

It may be tempting to achieve an increase in the initial methane fraction ($z_1^{(0)}$) by removing ethane. However, this can be counter-productive as it will increase η (and z_{leid}), and thus the maximum pressure p^*. Despite the increase in Leidenfrost fraction, the overall effect will still be to reduce the relative amount of remaining LNG at triggering (r), due to the increase in initial methane fraction.

According to this model, a more surefire way of reducing risk will be to reduce the amounts of the heavier hydrocarbons C3 and C4. This will ensure that both the pressure and energy yield of the vapor explosion is reduced. Only when these are down to very small fractions should one start removing C2 to further reduce risk.

7. Example

We now find the predictions of the model for a typical LNG composition. The quantitative results are shown in Tab. 3. Note that all the energy results are given in energy per amount of LNG. A single tank on an LNG carrier may hold around 20 000–30 000 $\mathrm{m^3}$ LNG, which is about $1 \cdot 10^7$ kg. When accounting for the boil-off before triggering, this is around $1 \cdot 10^5$ MJ of potential RPT vapor-explosion energy. Of course, this is unlikely to be released all in one explosion, but rather in multiple less powerful ones.

A different approach would be to assume that one liter (10 cm cube) of LNG is triggered at once. The mass of one liter of LNG right before triggering (bubble temperature at the Leidenfrost composition) is 0.651 kg, which when multiplied with $E^{(\mathrm{mass})}$ gives a yield of 48 kJ, or about 11 g TNT equivalent.

8. Consistency with experiments

8.1. Triggering criteria

Empirical criteria for RPT to occur with cryogens have been presented in the literature. While this ultimately depends on chemical composition, the criteria are typically presented in terms of relations between surface temperature and composition-dependent temperature properties of the cryogen. A commonly cited empirically based criterion is (Porteous and Reid, 1976; Reid, 1983; Hightower et al., 2004; Luketa-Hanlin, 2006)

$$1.0 < \frac{T_{\mathrm{w}}}{T_{\mathrm{SHL}}} < 1.1. \tag{22}$$

The left hand side of our theoretical criterion Eq. (1) trivially agrees with the left hand side inequality of Eq. (22). Regarding the right hand side, if we combine Eq. (3) with the mid-point of the interval in Eq. (10) ($T_{\mathrm{SHL}} \approx 0.77 T_{\mathrm{crit}}$), we find that

$$T_{\mathrm{leid}} \approx \frac{27}{32} \frac{T_{\mathrm{SHL}}}{0.77} \approx 1.1 T_{\mathrm{SHL}}. \tag{23}$$

Thus, the present model predicts the empirical observation in Eq. (22) and serves to explain its theoretical basis. The correspondence also serves as a validation of the present RPT triggering model.

On a more qualitative note, it has been reported that RPT will not occur when methane or ethane is spilled on water, but will occur if relatively small amounts of propane or butane are added (Enger et al., 1973; Porteous and Reid, 1976). This is correctly predicted by the present model, in which no RPT may occur when $\eta < 1.09$. Methane and ethane alone has $\eta = 1$, and the only way to increase η is to add heavier alkanes. For LNG-like mixtures, it has been shown that the methane fraction must be reduced to at least 40% for RPT to occur (Enger et al., 1973). This is consistent with the present model, which predicts $z_{\mathrm{leid}} < 0.5$ for the typical range of $\eta \in (1.1, 1.4)$, as seen in Fig. 6. See also the example in Fig. 5, which predicts almost exactly 40%.

8.2. RPT consequence

Quantifying RPT energy yield and pressure from experiments has proven to be much more difficult than simply noting under which conditions RPT occurs. Still, some sporadic data does exist. Reported RPT underwater peak pressures 1 m from the triggering point have been reported to be 7 bar (Porteous and Reid, 1976), 15 bar (Enger et al., 1973) or "order of tens of bars" (Cleaver et al., 1998). As seen in Fig. 9 the model predicts 25–55 bar for the typical range of $\eta \in (1.1, 1.4)$, which is both in the correct order of magnitude and a reasonable upper bound. The fact that the pressure prediction is on the high side does not necessarily mean that it is incorrect, as it represents peak pressure at the source. The pressure is expected to decay rapidly with distance (Cleaver et al., 1998; Bubbico and Salzano, 2009), so the actual source pressure may be significantly higher.

It has been claimed that peak pressure is a poor predictor for RPT destructiveness (Jazayeri, 1977). It seems likely that RPT energy yield plays a more important role. This has to our knowledge not been directly measured but has been estimated from other measurements. The yield of single RPT events have been estimated to have TNT equivalents from a few grams all the way up to 6 kg (about 25 MJ) (Cleaver et al., 1998; ABS Consulting, 2004; Hightower et al., 2004; Melhem et al., 2006; Koopman and Ermak, 2007). Most authors do not specify whether a yield estimate is for an early or delayed RPT event. From the few instances where it is specified, there seems to be no clear trend regarding which kind of RPT has the highest yield, though the highest reported yield (6 kg) were from an early RPT. Delayed RPTs seem to have yields anywhere from a few grams to 3 kg. It is not known if this variability is due to a varying yield per mass, or a varying amount of mass participating in the event. As seen in Fig. 10, the present model predicts a yield of about 50–80 kJ kg^{-1} for triggered LNG, which is about 10–20 g TNT equivalent per kg of LNG. Unfortunately, this cannot be compared directly to yields from actual RPT events because the amount of participating LNG in each single RPT event is unknown. Still, we may perform the following two consistency checks regarding the explosive yield:

- Use model to estimate total potential yield over multiple events: If we consider a limited LNG spill of 10 m^3 (about 5000 kg) with the composition of Tab. 3, we find from $E_0^{(\mathrm{mass})}$ that this spill has a potential yield of about 85 MJ (20 kg TNT) after boiling off. This is certainly sufficient to provide multiple RPT events on the scale of kg TNT, as seen in experiments.
- Use model to estimate participating amount in single events: Experiments report that single delayed RPT events can have yields from a few grams to 3 kg TNT. According to the present model the yield is 10–20 g TNT per kg of LNG, which implies that such events would require the participation of LNG volumes anywhere from about 1 L to 0.5 m^3. The majority of events are in the lower end of this this range, and such an amount surely seems reasonable given that events appear to occur in quite localized spots on the LNG pool.

While the above shows that the consequence model is reasonably consistent with observations, it is by no means a rigorous or conclusive validation. Such a thing would require additional experimental data, especially regarding the amount of LNG participating in single RPT events.

9. Conclusions

From established and reasonable assumptions a model for delayed LNG RPT based on thermodynamics and nucleation theory was developed. The model was then used to develop correlations which may be used without access to the underlying advanced algorithms. The model predicted the following general conclusions:

- Spilled LNG will typically boil down to about 10–20% of the original amount before triggering RPT. We found that the model is consistent with the often cited triggering criterion in Eq. (22).
- The RPT explosive yield per triggered LNG mass will generally be in the range 50–80 $\mathrm{kJ\,kg^{-1}}$, and this is quite independent of LNG parameters (Fig. 10). This yield is equivalent to 10–20 g TNT per kg LNG.
- Due to much of the LNG boiling off before triggering, the potential explosive yield per *spilled* mass will be in the range 5–60 $\mathrm{kJ\,kg^{-1}}$, but this is very dependent on LNG parameters (Fig. 11).
- The peak explosive pressure will generally be in the range of 20–60 bar, but this is very dependent on the alkane factor η (Fig. 9).
- Potential explosive yield and pressure may be reduced by decreasing the alkane factor η. This is achieved by reducing the alkanes heavier than ethane from the LNG (e.g. propane and butane).
- Potential explosive yield may be reduced by increasing the initial fraction of methane in the mixture. This should preferably be achieved by first removing components heavier than ethane, so as to not increase η.

The model is wholly dependent on the following two critical assumptions: That RPT triggering only occurs when passing a well defined Leidenfrost point and that the model Eq. (3) for the Leidenfrost point is accurate for mixtures. Both of these should be investigated more closely through film boiling experiments with alkane mixtures.

A significant shortcoming of the present model is its inability to predict the energy yield of single vapor-explosions. Since it is based on thermodynamics alone, it can only provide yields per a given amount. Predicting the amount of LNG participating in single events will require a different kind of model, likely involving fluid dynamics. A small scale experiment able to measure both explosive yield and the participating LNG amount per event would be extremely useful, not just for validating such a future model, but also for properly validating the present model's predictions for yield per mass. In general, more quantitative data on the consequence of cryogen RPT is sorely needed. The current available data is quite sparse.

Acknowledgements

This publication is based on results from the research project "Predicting the risk of rapid phase-transition events in LNG spills (Predict-RPT)", performed under the MAROFF program. The authors acknowledge the Research Council of Norway (244076/O80) for support.

References

ABS Consulting, 2004. Consequence assessment methods for incidents involving releases from liquefied natural gas carriers. Tech. Rep. GEMS 1288209, Report for the Federal Energy Regulatory Commission.
URL http://www.ferc.gov/industries/gas/indus-act/lng/cons-model/cons-model.pdf

Alderman, J. A., 2005. Introduction to LNG safety. Process Safety Progress 24 (3), 144–151.

Aursand, P., Gjennestad, M., Aursand, E., Hammer, M., Wilhelmsen, Ø., 2017. The spinodal of single- and multi-component fluids and its role in the development of modern equations of state. Fluid Phase Equilibria 436, 98–112.

Baumeister, K. J., Simon, F. F., 1973. Leidenfrost temperature– its correlation for liquid metals, cryogens, hydrocarbons, and water. (American Society of Mechanical Engineers, 1973.) ASME, Transactions, Series C- Journal of Heat Transfer, 95, 166–173.

Benintendi, R., Rega, S., 2014. A unified thermodynamic framework for lng rapid phase transition on water. Chemical Engineering Research and Design 92 (12), 3055–3071.

Berenson, P. J., 1961. Film-boiling heat transfer from a horizontal surface. Journal of Heat Transfer 83 (3), 351–356.

Bernardin, J. D., Mudawar, I., 1999. The Leidenfrost point: experimental study and assessment of existing models. Journal of Heat Transfer 121 (4), 894–903.

Berthoud, G., 2000. Vapor explosions. Annual Review of Fluid Mechanics 32 (1), 573–611.

Bubbico, R., Salzano, E., 2009. Acoustic analysis of blast waves produced by rapid phase transition of LNG released on water. Safety Science 47 (4), 515–521.

Cleaver, P., Humphreys, C., Gabillard, M., Nédelka, D., Heiersted, R., Dahlsveen, J., 1998. Rapid phase transition of LNG. In: 12th International Conference on Liquefied Natural Gas, LNG12. Perth, Australia.

Cleaver, P., Johnson, M., Ho, B., 2007. A summary of some experimental data on LNG safety. Journal of Hazardous Materials 140 (3), 429–438.

Enger, T., Hartman, D. E., Seymour, E. V., 1973. Explosive Boiling of Liquefied Hydrocarbon/Water Systems. Springer US, Boston, MA, pp. 32–41.

Fletcher, D. F., Theofanous, T. G., 1994. Recent progress in the understanding of steam explosions. Journal of Loss Prevention in the Process Industries 7 (6), 457 – 462.

Forte, K., Ruf, D., 2017. Safety challenges of LNG offshore industry and introduction to risk management. In: ASME 2017 36th International Conference on Ocean, Offshore and Arctic Engineering. American Society of Mechanical Engineers, pp. V03BT02A016–V03BT02A016.

Gottfried, B. S., Bell, K. J., 1966. Film boiling of spheroidal droplets. leidenfrost phenomenon. Industrial & Engineering Chemistry Fundamentals 5 (4), 561–568.

Havens, J., Spicer, T., 2007. United states regulations for siting LNG terminals: Problems and potential. Journal of Hazardous Materials 140 (3), 439 – 443.

Hicks, E. P., Menzies, D. C., 1965. Theoretical studies on the fast reactor maximum accident. In: Proceedings of Conference on Safety, Fuels and Core Design in Large Fast Power Reactors (ANL–7120). pp. 654–670.

Hightower, M., Gritzo, L., Luketa-Hanlin, A., 2005. Safety implications of a large lng tanker spill over water. Process safety progress 24 (3), 168–174.

Hightower, M., Gritzo, L., Luketa-Hanlin, A., Covan, J., Tieszen, S., Wellman, G., Irwin, M., Kaneshige, M., Melof, B., Morrow, C., Ragland, D., 2004. Guidance on risk analysis and safety implications of a large liquified natural gas (LNG) spill over water. Tech. Rep. Sandia Report SAND2004-6258, Sandia National Laboratories, Albuquerque, New Mexico.
URL http://prod.sandia.gov/techlib/access-control.cgi/2004/046258.pdf

Jazayeri, B., 1977. Impact cryogenic vapor explosions. Master's thesis, MIT.

Koopman, R., Ermak, D., 2007. Lessons learned from LNG safety research. Journal of Hazardous Materials 140, 412 – 428.

Kunz, O., Wagner, W., 2012. The GERG-2008 wide-range equation of state for natural gases and other mixtures: An expansion of GERG-2004. Journal of Chemical & Engineering Data 57 (11), 3032–3091.

Linstrom, P. J., Mallard, W. G. (Eds.), 2017. NIST Chemistry WebBook, NIST Standard Reference Database Number 69. National Institute of Standards and Technology, Gaithersburg MD, 20899.
URL http://webbook.nist.gov

Luketa-Hanlin, A., 2006. A review of large-scale LNG spills: Experiments and modeling. Journal of Hazardous Materials 132, 119 – 140.

Melhem, G., Saraf, S., Ozog, H., 2006. LNG properties and hazards, understanding LNG rapid phase transitions (RPT). An ioMosaic Corporation Whitepaper.

Michelsen, M. L., Mollerup, J. M., 2007. Thermodynamic models: Fundamentals and computational aspects, 2nd Edition. Tie-Line Publictions, Holte, Denmark.

Nagai, N., Nishio, S., 1996. Leidenfrost temperature on an extremely smooth surface. Experimental thermal and fluid science 12 (3), 373–379.

Nédelka, D., Sauter, V., Goanvic, J., Ohba, R., 2003. Last developments in rapid phase transition knowledge and modeling techniques. In: Offshore Technology Conference.

Peng, D.-Y., Robinson, D. B., 1976. A new two-constant equation of state. Industrial & Engineering Chemistry Fundamentals 15 (1), 59–64.

Pitblado, R. M., Woodward, J. L., 2011. Highlights of LNG risk technology. Journal of Loss Prevention in the Process Industries 24 (6), 827 – 836.

Porteous, W. M., Reid, R. C., 1976. Light hydrocarbon vapor explosions. Chem. Eng. Prog. Vol. 72:5, 83–89.

Qiao, Y. M., Chandra, S., 1997. Experiments on adding a surfactant to water drops boiling on a hot surface. In: Proceedings of the Royal Society of London A: Mathematical, Physical and Engineering Sciences. Vol. 453. The Royal Society, pp. 673–689.

Raj, P. K., Bowdoin, L. A., 2010. Underwater LNG release: Does a pool form on the water surface? What are the characteristics of the vapor released? Journal of Loss Prevention in the Process Industries 23 (6), 753 – 761.

Reid, R. C., 1983. Rapid phase transitions from liquid to vapor. In: Advances in Chemical Engineering. Vol. 12. pp. 105–208.

Sakurai, A., Shiotsu, M., Hata, K., 1990. Effects of system pressure on minimum film boiling temperature for various liquids. Experimental Thermal and Fluid Science 3 (4), 450–457.

Shaw, S., Baik, J., Pitblado, R., 2005. Consequences of underwater releases of lng. Process Safety Progress 24 (3), 175–180.

Soave, G., 1972. Equilibrium constants from a modified Redlich–Kwong equation of state. Chemical Engineering Science 27 (6),

1197–1203.
Span, R., 2010. Multiparameter Equations of State: An Accurate Source of Thermodynamic Property Data. Springer-Verlag, Berlin.
Spiegler, P., Hopenfeld, J., Silberberg, M., Bumpus, C. F., Norman, A., 1963. Onset of stable film boiling and the foam limit. International Journal of Heat and Mass Transfer 6 (11), 987–989.
Valencia-Chavez, J. A., 2 1978. The effect of composition on the boiling rates of liquefied natural gas for confined spills on water. Ph.D. thesis, Massachusetts Institute of Technology.
Vesovic, V., 2007. The influence of ice formation on vaporization of LNG on water surfaces. Journal of hazardous materials 140 (3), 518–526.
Wilhelmsen, Ø., Aasen, A., Skaugen, G., Aursand, P., Austegard, A., Aursand, E., Gjennestad, M., Lund, H., Linga, G., Hammer, M., 2017. Thermodynamic Modeling with Equations of State: Present Challenges with Established Methods. Industrial & Engineering Chemistry Research 56 (13), 3503–3515.
Yao, S.-C., Henry, R. E., 1978. An investigation of the minimum film boiling temperature on horizontal surfaces. Journal of Heat Transfer 100 (2), 260–267.